GEOPHYSICAL RESEARCH LETTERS, VOL. 10, NO. 12, PAGES 1141-1144, DECEMBER 1983

FAULT PLANE SOLUTIONS FOR MICROEARTHQUAKES INDUCED AT THE FENTON HILL HOT DRY ROCK GEOTHERMAL SITE: IMPLICATIONS FOR THE STATE OF STRESS NEAR A QUATERNARY VOLCANIC CENTER

Dan Cash, E. F. Homuth, Hans Keppler[1], Chris Pearson, and Sunji Sasaki[2]

Earth and Space Sciences Division, Los Alamos National Laboratory, Los Alamos, New Mexico 87545

Abstract. Fault plane solutions of earthquakes induced during attempts to stimulate two hot dry rock reservoirs at Fenton Hill have significantly different patterns of first motions. The fault plane solution for the lower reservoir indicates strike slip, either left lateral strike slip on a N-S vertical plane or right lateral slip on an E-W vertical plane. In contrast, the solution for the upper zone includes largely vertical slip on a N-S nearly vertical plane, or oblique slip on a nearly horizontal plane. Because the N-S nodal plane is common in both solutions we infer that this represents the true fracture plane. Faulting thus seems to occur on a series of parallel faults or joints that intersect both reservoirs but a change in the slip vector indicates a major change in the state of stress between the upper and lower reservoirs. This latter conclusion is surprising because the two reservoirs are separated by less than 1 km. We suggest that this rapid change in the stress field may be related to the structure and subsidence of the nearby Valles Caldera.

Introduction

At Los Alamos National Laboratory's Hot Dry Rock (HDR) Geothermal project at Fenton Hill, New Mexico, a concept for extracting heat from low permeability crystalline rock is being developed. A hot dry rock geothermal site consists of two wells connected at depth by a fracture system that acts as a downhole heat exchanger during energy extraction operations. As the HDR concept uses hydraulic fracturing for permeability enhancement, methods to monitor the fracture growth are important. One such method originated at Los Alamos is the mapping of microearthquakes induced by massive pumping (Albright and Hanold, 1976). High temperature three-component orientable acoustic borehole sondes have been developed for this purpose (Cremer et al., 1980).

This paper presents fault plane solutions of some of the larger microearthquakes which were induced during hydraulic fracturing experiments at Fenton Hill. During this study we observed two quite different fault plane solutions associated with two regions in the reservoir that are separated by less than 1 km. These results suggest very rapid changes in the state of stress near Fenton Hill, changes that may be related to the nearby Valles Caldera.

The new HDR system at Fenton Hill consists of two wells drilled 4600 m into granitic rock. The bottom 1100 m of each wellbore were directionally drilled to an angle of 35° from the vertical, the production well (EE-3) being placed 380 m above the lower injection well (EE-2). These wells are to be connected at depth by a fracture system that provides hydraulic communication between the wells and is to be tested as a downhole heat exchanger for energy extraction operations.

Locations of Induced Microearthquakes

The microearthquakes described here were induced during hydraulic fracturing in two widely separated zones in EE-2. The first and deepest group of events occurred during stimulations of the the bottom 137 m of EE-2 (4248-4385 m) and the upper group occurred during stimulation of a second higher zone in the same well (3460-3630 m). During both stimulations, through the use of cemented liners, packers and sandplugs, only the depth range of interest was exposed to high pressure water. Not surprisingly, hypocenters from each stimulation formed clusters that were separated from each other in space.

The larger of the induced microearthquakes at Fenton Hill (with magnitudes as large as +1/2) were recorded on a surface network consisting of eight temporary and five permanent stations. Each of the temporary and three of the permanent stations employed a single (vertical) Geotech S-500 geophone (1-100 Hz) and lay within 5 km of the epicentral region. Signals were telemetered back to a central recording facility at the geothermal site. In addition to this "close-in" network, two other more distant stations detected adequate signals to contribute to the analysis. Locations of all the stations used in this study are shown in Fig. 1. Stations at greater distances did not detect usable signals, in part because of the highly attenuating volcanic rock of the Caldera.

In addition to surface stations, during the hydraulic fracturing experiments we monitored seismic activity using a three-component downhole geophone package and located events using the techniques of single station seismometry described by Albright and Pearson (1982). Located at depth in a wellbore, between 200 m and 4 km from source regions and below the attenuating sediments it was much more sensitive than the surface array and recorded up to 250,000 signals per experiment, some with magnitudes as low as -5.

We compared event locations calculated from

[1] Visiting Scientist from Institute for Geosciences and Natural Resources (BGR), Hanover, Germany

[2] Visiting Scientist from Central Research Institute of Electric Power Industry (CRIEPI), Abiko, Japan

Paper number 3L1567.

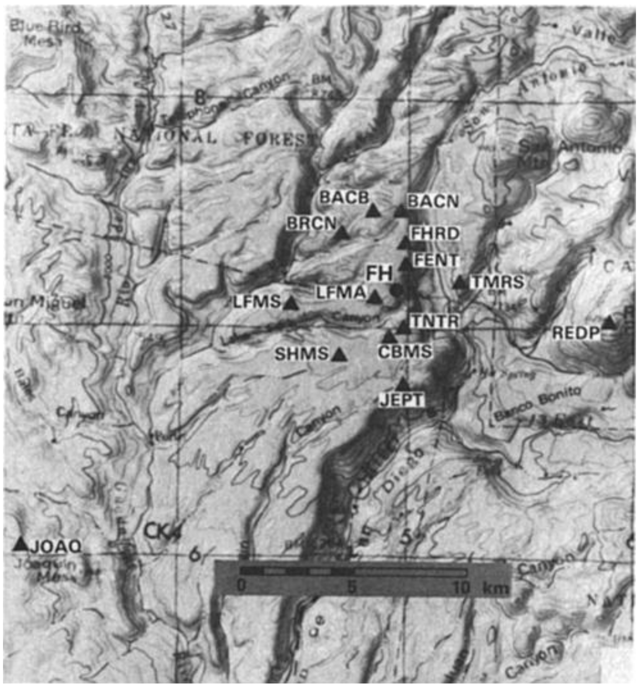

Fig. 1. Locations of seismic stations deployed near the Fenton Hill Hot Dry Rock Geothermal site. FH denotes the Fenton Hill hot dry rock site.

the three-component downhole seismic package with hypocenters of the larger events determined using first arrivals on the surface stations and a velocity structure for the region near Fenton Hill after Wechsler et al. (1980). The locations always agree within a few hundred meters. Figure 2 shows locations of some of the events induced by three hydraulic stimulations of the geothermal reservoir, two in the lower reservoir and one in the upper reservoir. In the lower reservoir, seismicity occurred on a well-defined planar zone that dips about 45° west and strikes about 20° west of north whereas events occurring during stimulation of the upper reservoir occurred in a much smaller, ellipsoidal volume that lacks notable structure. Note that the largest events induced at Fenton Hill were well dispersed in the seismic volumes defined by the more numerous smaller events. This suggests that the larger events occurred on a series of parallel joints distributed throughout the reservoir, not on a single fault. The 45° dipping seismically active zone in the lower reservoir probably is a permeable zone that allows high pressure water to disperse rapidly within a confined volume, causing fracturing along a set of nearly vertical planes as defined by the fault plane solutions. Hence the orientation of the seismic zone probably is independent of the fault plane orientations.

Fault Plane Solutions

The pattern of directions of first motion for microquakes was nearly consistent from within each reservoir, although the patterns for the two reservoirs were quite different. Therefore, we used composites of all the upper or lower data in each of the respective fault plane solutions illustrated in Figures 3 and 4. Note that in both cases we have plotted the first motions on the upper hemisphere. We made this choice because the stations are located very close to the epicenters of the events and the first arrivals will be upgoing rather than downgoing rays. The fault plane solution for the lower reservoir (Fig. 3) is a well constrained strike-slip solution, either right lateral strike slip on a vertical E-W plane or left lateral strike slip on a vertical N-S plane. The fault plane solution for the upper reservoir (Fig. 4) contains one fairly well-defined nodal line, once again a nearly vertical N-S striking plane (strike = N10°E, dip = 85°). The second plane is not well constrained by our data however, and several possible nodal planes are indicated in Fig. 4. No matter what we assume for the second nodal plane, slip on the N-S nodal plane must contain a substantial vertical component. In fact the slip vector on this plane must plunge at least 50° from the horizontal. If the poorly constrained nodal plane represents the fault plane, then we have largely horizontal motion of opposite sense to that of the lower fault plane solution. Thus a strike-slip solution, as inferred for the lower zone is not consistent with our data for the upper reservoir.

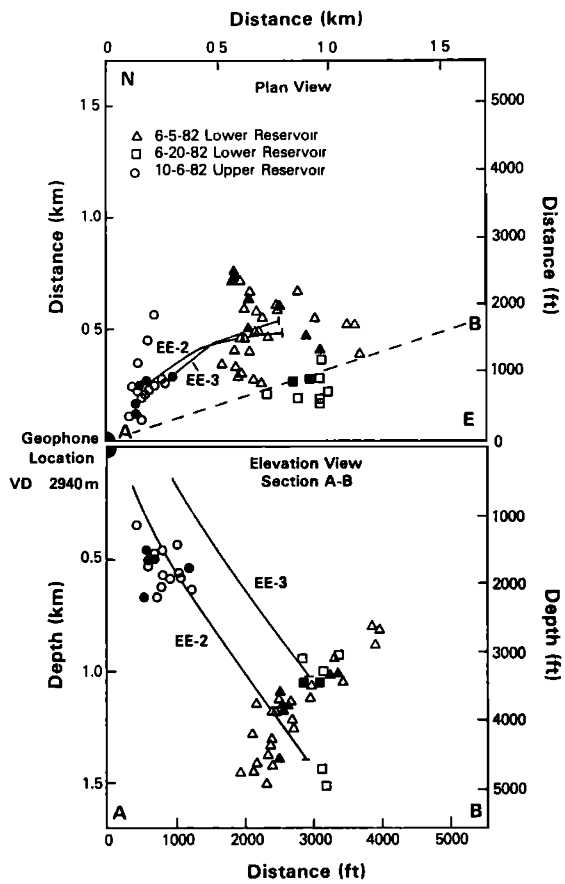

Fig. 2. Event locations from three hydraulic fracturing experiments that produced events large enough to be recorded on surface seismic stations.

Interpretation

The fault plane solutions are clearly distinct but a nearly vertical N-S trending nodal plane is present in both solutions. Because the solutions are similar in this respect and because N-S trending fracture orientations have been observed before, both during joint surveys (Laughlin et al., 1983) and during hydraulic fracturing experiments (Albright and Pearson, 1982), we think that the N-S plane represents the true fault plane.

Directions of the P and T axes are indicated in Figs. 3 and 4. For the lower reservoir the P axis is nearly horizontal, plunging slightly to the northwest while the T axis is also nearly horizontal, plunging slightly to the southwest. Because the second nodal plane is not well constrained in the upper reservoir, the P and T axes cannot be accurately determined for this solution. Regardless of our choice for the second nodal plane however, the P axis will be closer to the vertical in the upper reservoir, plunging to the east at an angle between 20 and 50 degrees. Hatched regions in Fig. 4 show the range of P and T axes with possible choices of the nodal planes. Note that a major difference between the P axes from the two solutions is the greater plunge of the P axis in the upper reservoir.

McKenzie (1969) shows that when earthquakes result from reactivation of pre-existing fractures the state of stress inferred from fault planes is not well constrained because the direction of rupture will be controlled by the orientation of pre-existing rupture planes. However, the slip vector must be parallel to the shear stress component acting in the fault plane because the shear stress is the agent that causes the blocks to move. If the fracture planes are the same in the upper and lower reservoir while the direction of slip is significantly different, the state of stress must also be different. The slip vector has a larger vertical component in the upper reservoir than is inferred in the lower reservoir, suggesting that the shear stress acting on surfaces that form the fault plane also has a larger vertical component in the upper reservoir than is the case 800 m lower.

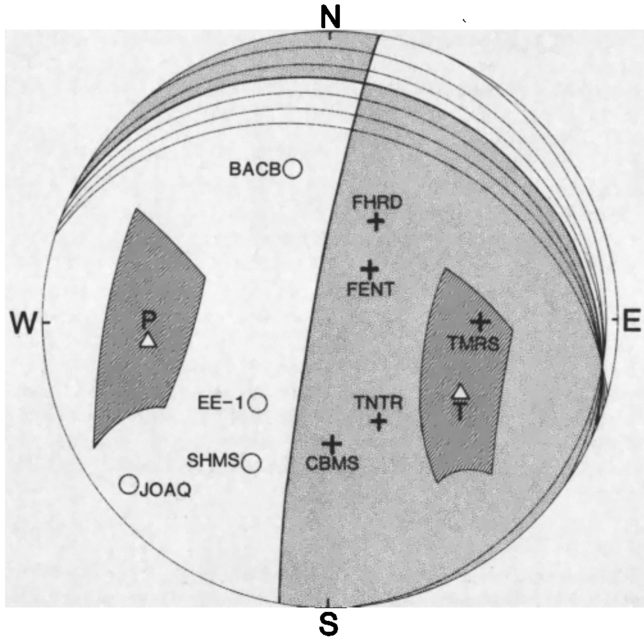

Fig. 4. Fault plane solution for the upper reservoir. Symbols have same meaning as in Fig. 3. Hatched regions indicate the range of P and T axes.

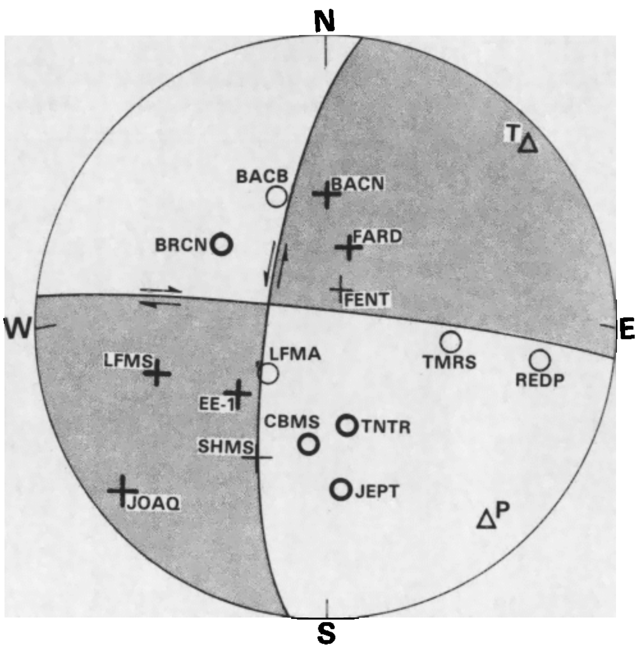

Fig. 3. Fault plane solution for the lower reservoir. Compressional first motions are indicated by plus symbols and dilatations by circles.

Conclusions

Taken together, two fault plane solutions for induced microearthquakes at a hot dry rock geothermal site imply that the state of stress changes considerably over a vertical distance of less than 1 km in the earth. Surprisingly the greatest principal stress changes from nearly horizontal in the deeper solution to an intermediate angle in the upper solution in spite of the fact that the overburden stress should be 21 MPa (210 bar) less at the upper reservoir than at the lower reservoir because of the difference in depth of burial. We can account for this seeming inconsistency by the fact that the Fenton Hill hot dry rock site lies near the boundary of the Valles Caldera. Because the geothermal wells were directionally drilled to the east, the lower reservoir is 450 m closer to the Caldera rim. The most likely explanation for the anomalously high horizontal stresses observed is that the lower reservoir is closer to a subsiding magma chamber under the Caldera which has been postulated by Smith et al. (1970). Anderson (1936) demonstrates that a subsiding magma chamber can cause anomalously large horizontal stresses due to arching in rocks overlying the chamber. This effect is strongest immediately above the chamber but persists at locations slightly off to the side. However, as the distance from the center of the chamber increases, the greatest principal stress trajectories begin to turn down. This model can be used to qualitatively explain our results because the lower reservoir, which is closer to the magma chamber, shows large horizontal stresses relative to those in the upper reservoir. The lower reservoir is nearly 1 km closer to the southwestern boundary of the chamber (inferred from the location of the ring fault), about 400 m horizontally and 700 m vertically.

Structural effects associated with the topographic rim of the caldera are another possible explanation for the anomalously high horizontal stresses. Jaeger and Cook (1971) show that structural effects near the base of cliffs can produce anomalously high horizontal stresses but it seems unlikely that this effect would persist in the lower reservoir which is nearly 3 km underneath the caldera rim.

The tension axis, inferred from the lower fault plane solution, is quite similar to previous estimates of the minimum compressive stress direction which were based on the orientation of hydraulic fracture planes (Pearson, 1981). However the hydraulic fracturing data come from experiments conducted in a nearby well 1.6 km higher and 1 km displaced laterally from the deep zone described here. Although both estimates suggest that the minimum stress direction is nearly horizontal and trends between 50° and 70° east of north, the disagreement with the mechanism of the upper reservoir implies substantial local variability. More observations are required to more fully characterize the stress field in the vicinity of the reservoirs.

Acknowledgments

We would like to thank Chester Painter and John Gonzales of the ESS-3 field support staff who assisted in placing the temporary seismic net used in this paper and John Stewart who provided the data processing. Thanks also to the ESS-6 field support group at Los Alamos National Laboratory and Mike Fehler and Carl Newton who reviewed this paper and made many helpful suggestions. This work was supported by the U.S. Department of Energy.

References

Albright, J. N., and R. J. Hanold, Seismic mapping of hydraulic fractures made in basement rocks, paper presented at the Second Annual ERDA Enhanced Oil and Gas Recovery Symposium, Energy Res. and Develop. Admin., Tulsa, Okla., 1976.

Albright, J. N. and C. F. Pearson, Acoustic emissions as a tool for hydraulic fracture locations: Experience at the Fenton Hill Hot Dry Rock site., Society of Petroleum Engineers Journal, 22, 523-530, 1982.

Anderson, E. M., The dynamics of the formation of cone-sheets, ring-dykes and caldron subsidences, Proceedings, Royal Society of Edinburgh, 56, 128-157, 1936.

Cremer, G., R. Duffield, M. Wilson, and M. Smith (Ed.), Hot dry rock geothermal energy development project annual report, fiscal year 1979, Los Alamos Sci. Lab. Rep. LA-8280-HDR, Los Alamos, NM, p. 166, 1980.

Jaeger, J. C., and N. Cook, Fundamentals of Rock Mechanics, p. 24, Chapman and Hall, London, 1971.

Laughlin, A. W., A. C. Eddy, R. Laney and M. J. Aldrich, Geology of the Fenton Hill New Mexico Hot Dry Rock Site, Journal of Volcanology and Geothermal Research 15, 21-41, 1983.

McKenzie, D. P., The relation between fault plane solutions for earthquakes and the directions of the principle stresses, Bulletin of the Seismological Society of America 59, 591-601, 1969.

Pearson, C. F., The relationship between microseismicity and high pore pressures during hydraulic stimulation experiment in low permeability granitic rock, Journal of Geophysical Research 86, 7855-7864, 1981.

Smith, R. L., R. A. Bailey, and C. S. Ross, Geologic map of the Jemez Mountains, New Mexico, Miscellaneous Geologic Investigations Map I-571, U.S. Geol. Surv., 1970.

Wechsler, D. J., D. J. Cash, K. H. Olsen, N. J. McFarland and J. J. Wolff, Earthquake Catalog for Northern New Mexco: September 1973-December 1979. Los Alamos National Laboratory progress report LA-8509-PR, 1980.

(Received July 15, 1983;
accepted September 19, 1983.)